

Observation of Plasmon–Polariton Modes in Two-Dimensional Electron Systems

I. V. Kukushkin^{1,*}, D. V. Kulakovskii^{1,2}, S. A. Mikhailov², J. H. Smet², and K. von Klitzing²

¹ Institute of Solid-State Physics, Russian Academy of Sciences, Chernogolovka, Moscow region, 142432 Russia

² Max-Planck-Institut für Festkörperforschung, 70569 Stuttgart, Germany

*e-mail: kukush@issp.ac.ru

Received March 24, 2003

A manifestation of retardation effects, which were predicted theoretically more than 35 years ago, is revealed for the first time in the plasma excitation spectrum of a two-dimensional electron system with a high electron mobility. It is shown that a significant decrease in the resonant plasma frequency due to a hybridization of the plasma and light modes is observed in zero magnetic field. An unusual dependence of the frequency of the hybrid cyclotron–plasmon mode on the magnetic field has been observed in a perpendicular magnetic field. The experimental results are in good quantitative agreement with the theory. © 2003 MAIK “Nauka/Interperiodica”.

PACS numbers: 71.36.+c; 73.20.Mf

Natural plasma oscillations in two-dimensional electron systems were predicted by Stern in 1967 [1] and were observed experimentally approximately 10 years later in the electron system on the surface of liquid helium [2] and in silicon metal–insulator–semiconductor structures [3, 4]. These and numerous subsequent experiments (see the reviews [5, 6]) quantitatively confirmed the phonon dispersion predicted in [1, 7]

$$\omega_p^2(q) = \frac{2\pi n_s e^2}{m^* \epsilon(q)} q, \quad (1)$$

where n_s and m^* are the concentration and the effective mass of two-dimensional electrons and $\epsilon(q)$ is the permittivity of the surrounding medium. Plasma excitations in a variety of semiconductor structures, such as silicon metal–insulator–semiconductor structures or GaAs/AlGaAs heterojunctions, were detected by IR spectroscopy. The plasmon wave vector (with a typical magnitude of 10^4 cm^{-1}) in these experiments was specified by the period of the metal lattice, which provided the interaction between plasma excitations and the electromagnetic field.

The plasmon spectrum described by Eq. (1) was obtained within the quasielectrostatic approximation. The electrodynamic effects on the spectrum of plasma oscillations were studied theoretically in the work by Stern and also in the subsequent publications [8–11]. Retardation effects become essential at small quasimomenta of plasmons, when their phase velocity approaches the velocity of light. For the typical parameters of GaAs/AlGaAs heterostructures, this occurs at $q = 10 \text{ cm}^{-1}$ and a frequency of 10–30 GHz. Some years

ago, two-dimensional plasmons could not be observed at such low frequencies, because the quality of the structures was poor and, for this reason, the linewidth of plasma resonances was about 100 GHz. In the last ten years the quality of the samples has been improved significantly: the mobility of two-dimensional electrons has been enhanced by several orders of magnitude, and the linewidth of plasma resonances has decreased down to 2–10 GHz. These improvements allow the plasma resonance to be studied at low frequencies and at small quasimomenta and open up possibilities for studying retardation effects. The theory [9] predicts that a system of high-mobility two-dimensional electrons must exhibit weakly damped hybrid plasmon–polariton modes (bound states of plasmons with light). However, these hybrid modes have not been observed experimentally until the present time. In this work, we report the observation of these plasmon–polariton modes and a study of their dispersion and properties in a perpendicular magnetic field.

We studied several single GaAs/AlGaAs quantum wells with both large and small concentrations of two-dimensional electrons (from $0.2 \times 10^{11} \text{ cm}^{-2}$ to $6.6 \times 10^{11} \text{ cm}^{-2}$). In all the structures, the well width was 25 nm, and the mobility of electrons varied from 0.3 to $5 \times 10^6 \text{ cm}^2 \text{ V}^{-1} \text{ s}^{-1}$. The linewidths of resonant microwave absorption in all the structures studied did not exceed 5 GHz and were 1 GHz in the best structures. This allowed us to measure the plasmon–cyclotron resonance at record low microwave frequencies (10–50 GHz). In order to measure the dimensional plasma resonance, we manufactured circular disks with diameters of 0.1, 0.2, 0.3, 0.4, 0.5, 0.6, 1, 2, and 3 mm [12, 13] and used the optical detection method based on the high

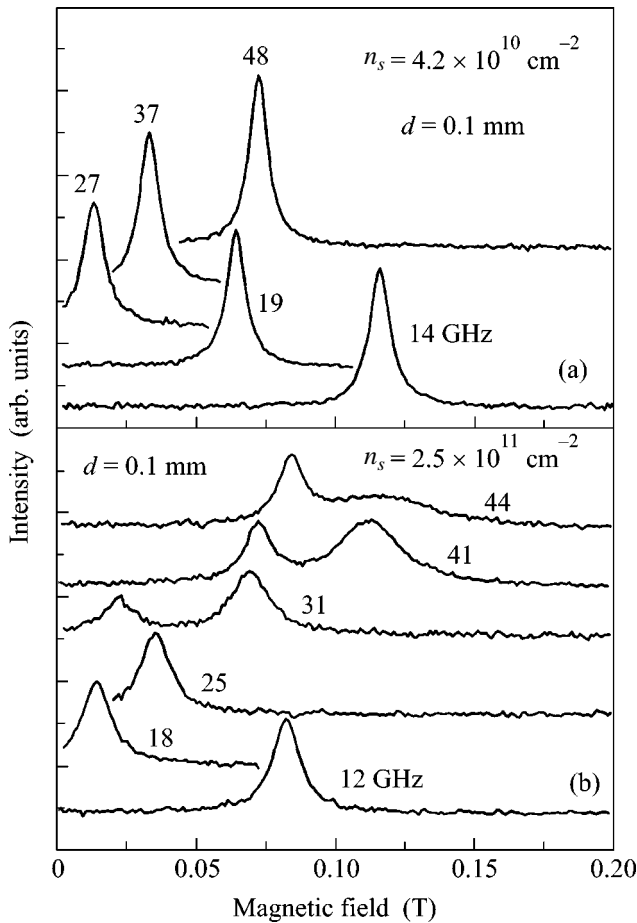


Fig. 1. Optically detected dimensional magnetoplasma resonance spectra of a two-dimensional electron gas measured at various microwave excitation frequencies for mesa structures with diameters (a) $d = 0.1$ mm and (b) $d = 1$ mm in a GaAs/AlGaAs quantum well with a well width of 250 Å.

sensitivity of luminescence spectra to heating of the two-dimensional electron system [14, 15]. The luminescence spectra were recorded using a CCD camera and a dual spectrometer, which provided a spectral resolution of 0.03 meV. A stabilized semiconductor laser with a wavelength of 750 nm and a power of 0.1 mW was used for photoexcitation. An HP-83650B generator was used as a source of microwave radiation in the range 10–50 GHz. The samples were placed at a maximum of the microwave electric field inside a 16-mm waveguide, which was short-circuited near the sample by a movable metal plug. The output microwave radiation power of the generator varied from 10 nW to 0.2 mW. The other experimental details can be found elsewhere [12, 13, 15]. Characteristic resonant absorption spectra for samples differing in the electron density and the mesa diameter are displayed in Fig. 1. The spectra exhibit both an edge magnetoplasmon (observed at low frequencies $\omega < \omega_p$) and a bulk magnetoplasmon (at $\omega > \omega_p$). The two-dimensional electron density was measured by the sensitive spectroscopic method, which

allowed the concentration to be measured to better than 10^{-3} . This was provided by an exceptionally small peak width in the spectrum of luminescence noise appearing in the quantum Hall effect regime at integer filling factors [16].

The magnetic-field dependence of the resonant absorption frequency measured for samples differing in the electron density and the mesa diameter is shown in Figs. 2a and 2b. When measuring the resonant absorption contour, we preferred to sweep the magnetic field at a fixed frequency rather than the reverse, because it was impossible to provide the constancy of the microwave power in the case of frequency sweep. The results obtained for two samples with a relatively small concentration of two-dimensional electrons ($0.46 \times 10^{11} \text{ cm}^{-2}$) and for small disk diameters (0.1 and 0.2 mm) are presented in Fig. 2a. The spectra measured demonstrate a typical pattern [17–20] of magnetoplasma absorption consisting of two modes, which were described in detail theoretically [17, 18, 21–24]. The frequency of the upper mode, which corresponds to the bulk magnetoplasmon, asymptotically tends to the cyclotron frequency in the limit of an infinite magnetic field. The frequency of the lower mode, which corresponds to the edge magnetoplasmon, tends to zero in the limit of strong magnetic fields. At $B = 0$, the frequencies of both modes coincide, and this frequency markedly differs from the frequency $\omega_0 = (2\pi n_s e^2 / m^* R \epsilon)^{1/2}$ (shown by an arrow in the figure), which follows from Eq. (1) if q in this equation is replaced by $1/R$.

The situation changes markedly if the dimensional magnetoplasma resonance is studied in samples with a high concentration of electrons and with a large mesa diameter. The results measured for a sample with $n_s = 2.54 \times 10^{11} \text{ cm}^{-2}$ and $d = 1$ mm are shown in Fig. 2b. In this figure, it is evident that several new features are observed at these parameters: (a) the resonance frequency measured at $B = 0$ is markedly lower than ω_0 ; (b) the slope $|d\omega_{\pm}/d\omega_c|$ at $B \rightarrow 0$ is significantly smaller than the standard value 1/2; and (c) at a certain finite value of the magnetic field, the upper magnetoplasma mode intersects the line corresponding to the cyclotron resonance and demonstrates a strange zigzag behavior, which is accompanied by the appearance of one more high-frequency mode. After crossing the cyclotron resonance line, the width of the absorption line starts to increase markedly, as is evident in Fig. 1. A further increase in the electron density and (or) in the mesa diameter leads to an even stronger manifestation of the above features [25].

A simple qualitative analysis allowed us to suggest that the observed phenomena are associated with retardation effects. Actually, the dimensionless parameter $A = \omega_0 \sqrt{\epsilon} R/c$, defined as the ratio of the plasmon frequency to the frequency of light with the same wave vector $q = 1/R$, can serve as an indicator of the degree

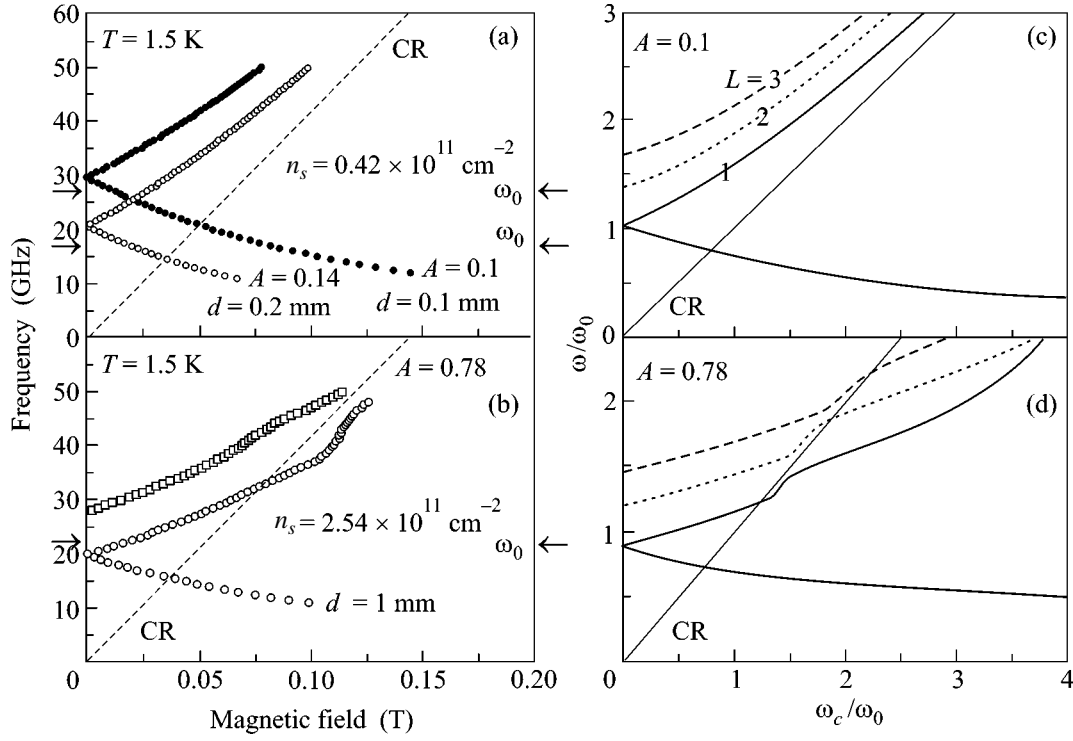


Fig. 2. Field dependence of magnetoplasma resonances: (a) and (b) experimental results obtained for samples with different electron densities and different mesa diameters; (c) and (d) theoretical calculations of the lowest ($n = 1$) modes with $L = 1, 2$, and 3 for parameters A obtained experimentally. Edge magnetoplasma modes for $L = 2$ and 3 are not shown on the plots.

of importance of retardation effects. This parameter grows with increasing n_s and R , because $A \sim \sqrt{n_s R}$, and it has never exceeded 0.1–0.15 in all the previous experimental studies. For the two samples shown in Fig. 2a, parameter A equaled 0.1 and 0.14 for diameters $d = 0.1$ and $d = 0.2$ mm, respectively, so that no manifestation of the finite velocity of light could be expected in the spectra. On the contrary, for the case shown in Fig. 2b, parameter A equaled 0.78; therefore, it was reasonable to associate the observed phenomena with retardation effects. In order to corroborate this assumption, we carried out calculations of the resonant magnetoplasma modes in a two-dimensional disk.

The electrostatic potential $\varphi(\mathbf{r}, z)$ and the vector potential $\mathbf{A}(\mathbf{r}, z)$ over all space must obey the Maxwell equations

$$\begin{aligned} \Delta \mathbf{A}(\mathbf{r}, z) - \frac{1}{c^2} \frac{\partial^2 \mathbf{A}(\mathbf{r}, z)}{\partial t^2} &= -\frac{4\pi}{c} \mathbf{j}(\mathbf{r}) \delta(z), \\ \Delta \varphi(\mathbf{r}, z) - \frac{1}{c^2} \frac{\partial^2 \varphi(\mathbf{r}, z)}{\partial t^2} &= -4\pi \rho(\mathbf{r}) \delta(z). \end{aligned} \quad (2)$$

Let us make the Fourier transformation with respect to variables (\mathbf{r}, t) . Using the known relations between the

current in a two-dimensional electron gas, the electron density, and the total electric field in the plane $z = 0$

$$\begin{aligned} j_\alpha(r, \theta) &= \sigma_{\alpha\beta}(r, \theta) E_\beta^{\text{tot}}(r, \theta), \\ \partial \rho / \partial t + \text{div } \mathbf{j} &= 0, \end{aligned} \quad (3)$$

for the cylindrically symmetric case, when the eigenmodes of the system are characterized by the angular momentum l and the radial quantum number n (see [18, 22, 26–28]), we obtain the following system of equations from Eqs. (2):

$$\begin{aligned} E_{r,l}^{\text{ind}}(r) &= \frac{2\pi i \omega}{c^2} \int_0^\infty \frac{q dq}{\chi_{q\omega}} J_{|l|}(qr) \int_0^\infty r' dr' J_{|l|}(qr') \\ &\times [\sigma_{rr}(r') E_{r,l}^{\text{tot}}(r') + \sigma_{r\theta}(r') E_{\theta,l}^{\text{tot}}(r')] \\ &- \frac{2\pi}{i\omega} \frac{\partial}{\partial r} \int_0^\infty \frac{q dq}{\chi_{q\omega}} J_{|l|}(qr) \int_0^\infty r' dr' J_{|l|}(qr') \\ &\times \left\{ \frac{1}{r'} \frac{\partial}{\partial r'} (r' [\sigma_{rr}(r') E_{r,l}^{\text{tot}}(r') + \sigma_{r\theta}(r') E_{\theta,l}^{\text{tot}}(r')]) \right. \\ &\left. + \frac{il}{r'} [\sigma_{\theta r}(r') E_{r,l}^{\text{tot}}(r') + \sigma_{\theta\theta}(r') E_{\theta,l}^{\text{tot}}(r')] \right\}, \end{aligned} \quad (4)$$

$$E_{\theta,l}^{\text{ind}}(r) = \frac{2\pi i \omega}{c^2} \int_0^\infty \frac{q dq}{\chi_{q\omega}} J_{|l|}(qr) \int_0^\infty r' dr' J_{|l|}(qr')$$

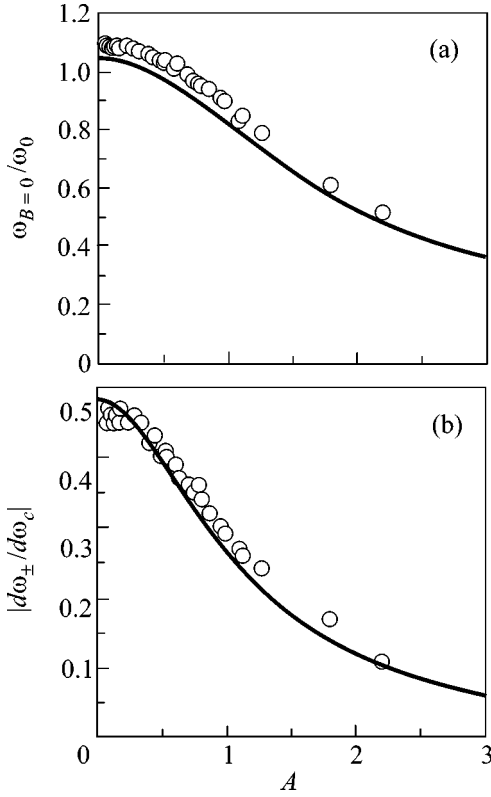


Fig. 3. (a) Normalized resonance frequency $\omega_{B=0}/\omega_0$ at $B = 0$ and (b) its slope $|d\omega_{\pm}/d\omega_c|$ at $B \rightarrow 0$ as functions of the dimensionless parameter $A = \omega_0 \sqrt{\epsilon} R/c$, $\omega_0 = (2\pi n_s e^2/m^* R \epsilon)^{1/2}$. Experimental data are shown by circles, and theoretical data are shown by a solid line.

$$\begin{aligned} & \times [\sigma_{\theta r}(r') E_{r,l}^{\text{tot}}(r') + \sigma_{\theta\theta}(r') E_{\theta,l}^{\text{tot}}(r')] \\ & - \frac{2\pi i l}{i\omega r} \int_0^{\infty} \frac{q dq}{\chi_{q\omega}} J_{|l|}(qr) \int_0^{\infty} r' dr' J_{|l|}(qr') \\ & \times \left\{ \frac{1}{r'} \frac{\partial}{\partial r'} (r' [\sigma_{rr}(r') E_{r,l}^{\text{tot}}(r') + \sigma_{r\theta}(r') E_{\theta,l}^{\text{tot}}(r')]) \right. \\ & \left. + \frac{il}{r'} [\sigma_{\theta r}(r') E_{r,l}^{\text{tot}}(r') + \sigma_{\theta\theta}(r') E_{\theta,l}^{\text{tot}}(r')] \right\}, \end{aligned}$$

with the accessory condition for the radial current component at the disk edge

$$j_r = \sigma_{rr}(R) E_{r,l}^{\text{tot}}(R) + \sigma_{r\theta}(R) E_{\theta,l}^{\text{tot}}(R) = 0. \quad (5)$$

By analogy with [22], we solved the system of Eqs. (4) with the additional condition (5) by the method of decomposing the unknown components of the total electric field $E_{r,l}^{\text{tot}}(r)$ and $E_{\theta,l}^{\text{tot}}(r)$ in an orthonormalized basis set and determined the magnetic-field depen-

dences for the magnetoplasmon energies in a disk with a stepped potential profile. The lowest ($n = 1$) mode with $L \equiv |l| = 1, 2$, and 3 for the parameters A obtained experimentally is presented in Figs. 2c and 2d. It is evident that the theory and experiment are in good agreement. A quantitative comparison of the measured and calculated frequencies allowed us to infer that the upper bulk magnetoplasma mode observed at $A = 0.78$ was the mode with the higher angular momentum $L = 2$ and the lowest $n = 1$ (modes with $n > 1$ have high frequencies).

Further we will concentrate on the quantitative analysis of our results in the region of small magnetic fields $B \rightarrow 0$. The dependence of the ratio $\omega_{B=0}/\omega_0$ on the parameter A measured for seven samples with various concentrations and radii is presented in Fig. 3a. This ratio starts from 1.1 at small values of A and decreases down to 0.5 as A increases up to 2.20. The solid line in the figure represents the results of theoretical calculations. At $A = 0$, our result coincides with the result obtained by Fetter [22] in the quasistatic approximation. The theory and experiment are in good agreement, and the small ($\sim 4\%$) discrepancy can be related to the inaccuracy of the determination of the effective dielectric constant $\bar{\epsilon}$ of the medium, which in the real system can depend on the size of the sample, the presence of the waveguide, etc. Figure 3b demonstrates the dependence of the slope $|d\omega_{\pm}/d\omega_c|$ at $B \rightarrow 0$ on the parameter A . It is readily seen that the slope is even more sensitive to an enhancement of retardation effects. An increase in the dimensionless parameter from 0 to 2.2 leads to a decrease in the slope by a factor of 4. The theoretical results shown in this figure with a solid line are in very good agreement with the experiment.

Finally, we will analyze our experimental data in order to qualitatively verify the two-dimensional plasmon dispersion $\omega(q)$ predicted in the pioneering work by Stern [1]. According to this work, the dispersion with regard to retardation effects takes the form

$$q^2 = \epsilon \omega^2/c^2 + \left(\frac{\omega^2}{2\pi n_s e^2/m^* \bar{\epsilon}} \right)^2. \quad (6)$$

Knowing the relation between the wave vector and the disk diameter ($q = 2.4/d$, see [25]), we can now obtain the resonance frequency as a function of the inverse mesa diameter. Such curves are shown in Figs. 4a and 4b for two different electron densities ($n_s = 6.6 \times 10^{11} \text{ cm}^{-2}$ and $n_s = 2.5 \times 10^{11} \text{ cm}^{-2}$). For comparison, we also depicted the dispersion of light $\omega = 2\pi f = cq/\sqrt{\epsilon}$ and the two-dimensional plasmon dispersion defined by Eq. (1). This figure confirms the validity of Eq. (6), because the dispersion of the hybrid mode at low concentrations primarily corresponds to the purely two-dimensional plasmon dispersion and approaches the dispersion of light at high densities in the region of small wave vectors. This fact is in perfect agreement

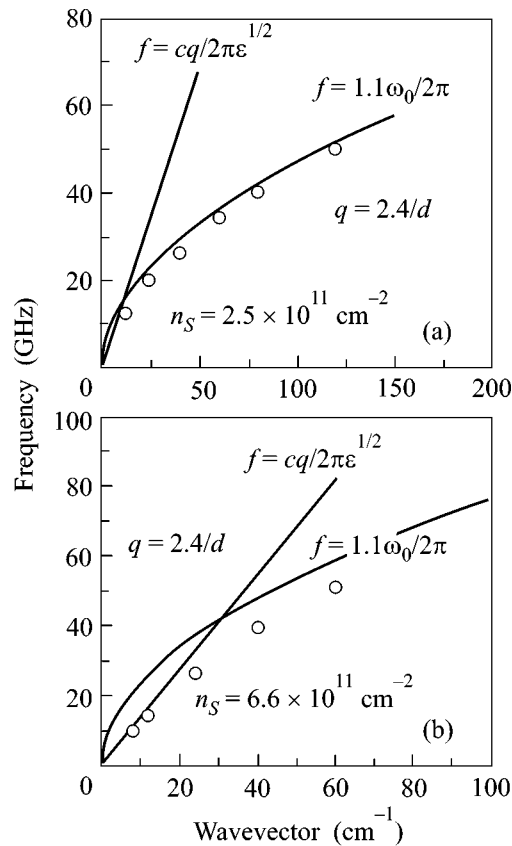


Fig. 4. Circles show the two-dimensional plasmon-polariton dispersion obtained from experimental data for two samples with different electron densities: (a) $n_s = 2.5 \times 10^{11} \text{ cm}^{-2}$ and (b) $n_s = 6.6 \times 10^{11} \text{ cm}^{-2}$. The dispersion of light is depicted by a straight line, and the two-dimensional plasmon dispersion is presented in the quasistatic approximation (Eq. (1)).

with the results obtained in [1, 9], in which it was shown that mixing between the plasma and light modes occurs only at high electron concentrations.

In this work, the absorption spectra of two-dimensional magnetoplasmons were studied at small wave vectors and in the region of low frequencies, where retardation effects must be manifested. The features associated with these effects were observed experimentally and explained theoretically. It should be noted separately that an anomalous hybrid magnetoplasma mode with a very unusual field dependence was observed in the region of finite perpendicular magnetic fields. The experimental results were compared with theoretical predictions for 2D plasmon-polaritons in an infinite two-dimensional electron gas at $B = 0$ and also for a disk-shaped sample in zero and finite magnetic fields. These calculations describe the experimental results well.

This work was supported by the Russian Foundation for Basic Research and INTAS.

REFERENCES

1. F. Stern, Phys. Rev. Lett. **18**, 546 (1967).
2. C. C. Grimes and G. Adams, Phys. Rev. Lett. **36**, 145 (1976).
3. S. J. Allen, Jr., D. C. Tsui, and R. A. Logan, Phys. Rev. Lett. **38**, 980 (1977).
4. T. N. Theis, J. P. Kotthaus, and P. J. Stiles, Solid State Commun. **26**, 603 (1978).
5. T. N. Theis, Surf. Sci. **98**, 515 (1980).
6. D. Heitmann, Surf. Sci. **170**, 332 (1986).
7. A. V. Chaplik, Zh. Éksp. Teor. Fiz. **62**, 746 (1972) [Sov. Phys. JETP **35**, 395 (1972)].
8. K. W. Chiu and J. J. Quinn, Phys. Rev. B **9**, 4724 (1974).
9. V. I. Fal'ko and D. E. Khmel'nitskiĭ, Zh. Éksp. Teor. Fiz. **95**, 1988 (1989) [Sov. Phys. JETP **68**, 1150 (1989)].
10. A. O. Govorov and A. V. Chaplik, Zh. Éksp. Teor. Fiz. **95**, 1976 (1989) [Sov. Phys. JETP **68**, 1143 (1989)].
11. S. A. Mikhaĭlov, Pis'ma Zh. Éksp. Teor. Fiz. **57**, 570 (1993) [JETP Lett. **57**, 586 (1993)].
12. S. I. Gubarev, I. V. Kukushkin, S. V. Tovstonog, *et al.*, Pis'ma Zh. Éksp. Teor. Fiz. **72**, 469 (2000) [JETP Lett. **72**, 324 (2000)].
13. M. Y. Akimov, I. V. Kukushkin, S. I. Gubarev, *et al.*, Pis'ma Zh. Éksp. Teor. Fiz. **72**, 662 (2000) [JETP Lett. **72**, 460 (2000)].
14. B. M. Ashkinadze and V. I. Yudson, Phys. Rev. Lett. **83**, 812 (1999).
15. I. V. Kukushkin, J. H. Smet, K. von Klitzing, and W. Wegscheider, Nature **415**, 409 (2002).
16. O. V. Volkov, I. V. Kukushkin, M. V. Lebedev, *et al.*, Pis'ma Zh. Éksp. Teor. Fiz. **71**, 558 (2000) [JETP Lett. **71**, 383 (2000)].
17. S. J. Allen, Jr., H. L. Störmer, and J. C. M. Hwang, Phys. Rev. B **28**, 4875 (1983).
18. D. C. Glattli, E. Y. Andrei, G. Deville, *et al.*, Phys. Rev. Lett. **54**, 1710 (1985).
19. T. Demel, D. Heitmann, P. Grambow, and K. Ploog, Phys. Rev. Lett. **64**, 788 (1990).
20. W. Hansen, J. P. Kotthaus, and U. Merkt, Semicond. Semimet. **35**, 279 (1992).
21. R. P. Leavitt and J. W. Little, Phys. Rev. B **34**, 2450 (1986).
22. A. L. Fetter, Phys. Rev. B **33**, 5221 (1986).
23. V. A. Volkov and S. A. Mikhaĭlov, Zh. Éksp. Teor. Fiz. **94**, 217 (1988) [Sov. Phys. JETP **67**, 1639 (1988)].
24. S. A. Mikhailov, Phys. Rev. B **54**, 10335 (1996).
25. I. V. Kukushkin, J. H. Smet, S. A. Mikhailov, and D. V. Kulakovskii, Phys. Rev. Lett. (in press).
26. S. S. Nazin and V. B. Shikin, Fiz. Nizk. Temp. **15**, 227 (1989) [Sov. J. Low Temp. Phys. **15**, 127 (1989)].
27. V. Shikin, S. Nazin, D. Heitmann, and T. Demel, Phys. Rev. B **43**, 11903 (1991).
28. Z. L. Ye and E. Zaremba, Phys. Rev. B **50**, 17217 (1994).

Translated by A. Bagatur'yants